Eurographics Conference on Visualization (EuroVis) (2014)
N. Elmqvist, M. Hlawitschka, and J. Kennedy (Editors)

Visualizing Uncertainty in HARDI Tractography Using Superquadric Streamtubes

V. Wiens[1], L. Schlaffke[2], T. Schmidt-Wilcke[2], T. Schultz[1,3]

[1]University of Bonn, Germany [2]University Hospital Bergmannsheil, Bochum, Germany [3]MPI for Intelligent Systems, Tübingen, Germany

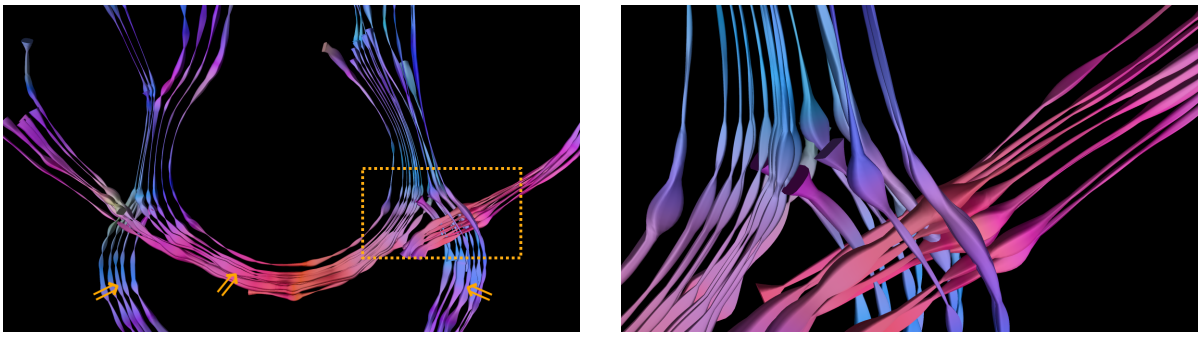

Figure 1: *Our superquadric streamtubes are wider in regions where the tracking direction is less certain; moreover, if uncertainty is largest in a particular direction (highlighted by arrows), they develop sharp edges which indicate that direction. The figure on the right presents a closeup view of the crossing fiber region marked by a dotted box in the left image.*

Abstract

Standard streamtubes for the visualization of diffusion MRI data are rendered either with a circular or with an elliptic cross section whose aspect ratio indicates the relative magnitudes of the medium and minor eigenvalues. Inspired by superquadric tensor glyphs, we propose to render streamtubes with a superquadric cross section, which develops sharp edges to more clearly convey the orientation of the second and third eigenvectors where they are uniquely defined, while maintaining a circular shape when the smaller two eigenvalues are equal. As a second contribution, we apply our novel superquadric streamtubes to visualize uncertainty in the tracking direction of HARDI tractography, which we represent using a novel propagation uncertainty tensor.

Categories and Subject Descriptors (according to ACM CCS): Computer Graphics [I.3.8]: Applications—

1. Introduction

In diffusion MRI (dMRI), the diffusion of water is measured to infer direction and microstructural properties of nerve fiber bundles in the human brain. The diffusion tensor, a symmetric 3×3 matrix, is the simplest model that captures this data [BMLB94], and streamtubes are one of the most widely used tools for visualizing it [VZKL06]. While their trajectory follows the principal eigenvector of the diffusion tensor, their cross section is either chosen to be circular or an ellipse that additionally encodes the directions of the medium and minor eigenvector and the ratios of the corresponding eigenvalues [DH93, ZDL03]. Inspired by the success of superquadric tensor glyphs in a range of applications [KWL*04, JKM06, KW06, HSSK14], in Section 3 of this paper, we propose a method that renders streamtubes with a superquadric instead of an elliptic cross section. As shown in Figure 4, this more clearly conveys medium and minor eigenvector directions.

High Angular Resolution Diffusion Imaging (HARDI) can be used to track through regions in which, due to par-

DOI: 10.2312/eurovisshort.20141154

tial voluming or fiber crossings, multiple fiber directions are present, and the diffusion tensor model is insufficient [TML11]. Recently, estimating and visualizing the uncertainty in tractography has been identified as a topic that still requires more attention [SVBK14].

In Section 4, we contribute to these two topics by proposing a method to quantify the local uncertainty in the HARDI tracking direction. As shown in Figure 1, this uncertainty itself is often anisotropic – it can be considerably higher in some directions than in others – which is clearly visualized for the first time by our novel superquadric streamtubes.

2. Related Work

Efforts to improve streamlines and streamtubes have focused on hardware-accelerated [SGS05, RBE*06, MSE*06, PFK07] or illustrative rendering [EBRI09]. In contrast, we propose a new type of streamtube geometry which makes it easier to assess the anisotropy orthogonal to its trajectory. In the simplest case, that orthogonal anisotropy reflects the medium and minor eigenvectors of a diffusion tensor. However, we also demonstrate examples in which our new streamtube geometry effectively visualizes a new measure of uncertainty in multi-fiber HARDI tractography.

Existing work on visualizing uncertainty in dMRI tractography has recently been surveyed by Schultz et al. [SVBK14]. It includes methods that derive and visualize tract confidence intervals [STS07, BPtHRV13, BBH14], and that allow the user to explore parameter sensitivity [BVPtHR09]. Most closely related to our work is PASTA ("Pointwise Assessment of Streamline Tractography Attributes") [JTE*05], which scales the diameter of a streamtube according to the width of the 95% confidence interval of inferred fiber directions. However, unlike our method, PASTA is only designed for single-fiber tractography based on the diffusion tensor model, and it visualizes the uncertainty as being isotropic in the plane orthogonal to the main direction. In contrast, our results demonstrate that the uncertainty in fiber tractography often has a significant main direction, which is clearly visualized by the superquadric cross sections of our streamtubes.

Our method should not be confused with recently proposed hyperstreamlines that indicate secondary fiber compartments which cross the one whose trajectory is being visualized [VVL13]. Those resemble the continuous placement of ODF glyphs along the trajectory [PPvA*11], whereas we visualize the uncertainty in the propagation direction, not the presence of secondary fiber compartments.

3. Superquadric Streamtubes

We will first explain how to create superquadric streamtubes from the diffusion tensor model, with sorted eigenvalues $\lambda_1 \geq \lambda_2 \geq \lambda_3 \geq 0$ and corresponding eigenvectors $\mathbf{e}_i$. In this setting, the trajectory of the streamtube is given by integrating the principal eigenvector direction, and the medium and minor eigenvectors, along with the corresponding eigenvalues, define the shape of its cross section. The modifications required for HARDI uncertainty visualization are presented separately, in Section 4.

3.1. Sampling the Superquadric Cross-Sections

Similar to superquadric tensor glyphs [Kin04], it is our goal to generate streamtubes whose cross section is circular when $\lambda_2 = \lambda_3$, indicating the fact that, in this case, $\mathbf{e}_2$ and $\mathbf{e}_3$ can be freely rotated in the plane orthogonal to $\mathbf{e}_1$. As the ratio of λ_2/λ_3 becomes smaller, the cross section should smoothly transition into a square shape whose sharp edges clearly indicate the directions of the now well-separated medium and minor eigenvectors. Even though, for clarity, the illustrations in Figures 2 and 3 show squares, this section explains how to create streamtubes that smoothly transition between square and circular shapes, as they are shown in Figure 1.

For each streamtube vertex $\mathbf{x}$, we generate a cross section by first creating a superquadric in the y-z-plane with its center at the origin. We then scale this geometry, align it by multiplication with a rotation matrix $\mathbf{R}$, and translate it to $\mathbf{x}$.

Initial superquadrics are created using the parametrization given by Löffelmann and Gröller [LG95], which obtains a point on the shape as a function

$$f(\theta,\rho) = \begin{pmatrix} 0 \\ \rho(\theta,\sigma')\cos(\theta) \\ \rho(\theta,\sigma')\sin(\theta) \end{pmatrix} \tag{1}$$

of angle θ and radius

$$\rho(\theta,\sigma') = \left((cos^2\theta)^{\frac{1}{\sigma'}} + (sin^2\theta)^{\frac{1}{\sigma'}} \right)^{-\frac{\sigma'}{2}}, \tag{2}$$

where we use the ratio $\sigma = \lambda_3/\lambda_2 \in [0,1]$ of the diffusion tensor eigenvalues and an additional sharpening factor γ, similar to the one used by Kindlmann [Kin04], to arrive at the final superquadric shape parameter $\sigma' = \sigma^\gamma$. Results shown in this paper use $\gamma = 3$. In the limit of $\sigma' \to 0$, the superquadric shape becomes a square. Since using Eq. (2) directly would be numerically unstable, we employ basic trigonometric relationships on the unit square to derive the value of ρ in this case.

Scaling of this base geometry can be done in two ways: The first option is to keep the maximal radius of the streamtube constant, but to still convey the eigenvalue ratio σ, as in [ZDL03]. This is achieved by scaling the z-component of Eq. (1), which represents the minor eigenvector direction, with σ. For uncertainty visualization, we prefer a variable radius to visualize the changing overall amount of uncertainty. In this case, we scale y by λ_2, and z by λ_3. In both cases, scaling factors smaller than some minimum ε are clamped to ε to maintain visibility of the streamtube, and a user-defined global scaling factor is applied. Finally, the rotation matrix

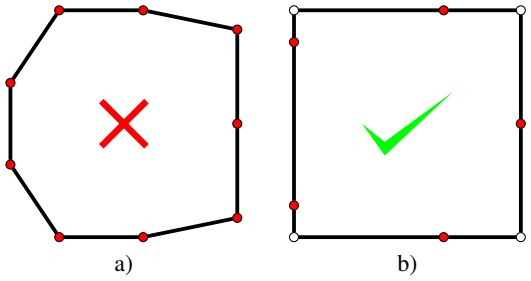

Figure 2: *a) Uniform sampling of a square with 9 points at angular distance $\alpha = (2\pi/9) = 40^\circ$ cuts off corners. b) Our method always samples the white corner points; additional red points are placed at $k \cdot (2\pi/5) = k \cdot 72^\circ$.*

is given as $\mathbf{R} = (\mathbf{e}_1|\mathbf{e}_2|\mathbf{e}_3)$, where $\mathbf{e}_i$ are the eigenvectors of the diffusion tensor.

Suitable sampling is crucial for a good visual appearance of the streamtube. In Figure 2 a), a unit square is sampled with $n = 9$ points that are equally distributed on $[0, 2\pi]$, resulting in a deformed shape. To achieve more robust results, we always sample the four corners first. The remaining points are distributed equally with angular distance $\alpha = \frac{2\pi}{n-4}$. If, for some k, $k\alpha$ is a multiple of 45°, we replace it with $k\frac{2\pi}{n-4+1}$ to avoid a repeated sampling of the corners.

3.2. Generating a Streamtube Mesh

A mesh representation of the streamtube is computed by connecting the planar cross sections with triangle strips. For square shapes, we create the connection between subsequent cross sections based on the corners of the geometry, since this results in an optimal representation of twisting fibers.

One corner $\mathbf{p}_c^1$ of the first plane G^1 is projected into the adjacent plane G^2, producing point $\mathbf{p}'_c$. In the plane G^2, the corner point $\mathbf{p}_c^2$ that minimizes the distance to $\mathbf{p}'_c$ is found. We then connect $\mathbf{p}_c^1$ to $\mathbf{p}_c^2$, and subsequent points accordingly, as illustrated in Figure 3 b). In contrast, as shown in Figure 3 a), simply connecting p_c^1 to the closest point on G^2 might connect corner points to points closer to the center of an edge, with undesirable visual results. For nearly circular shapes without pronounced corners ($\sigma' > 0.85$), we use the closest point on G^2 as the more appropriate alternative.

Figure 4 compares circular, elliptic, and superquadric streamtubes for DTI visualization. The superquadric cross sections in (c) most clearly show the twisting of the medium and minor eigenvectors as fibers from the corpus callosum turn toward the cortex. The figures use the red-to-white color coding proposed by Zhang et al. [ZDL03] to enhance visualization of the eigenvalue ratio ($\sigma = 0$: red, $\sigma = 1$: white).

For visualizations such as Figure 1, we achieve interactive framerates – 40 fps on a 1200×680 viewport – using a standard laptop (GeForce GTX 660M).

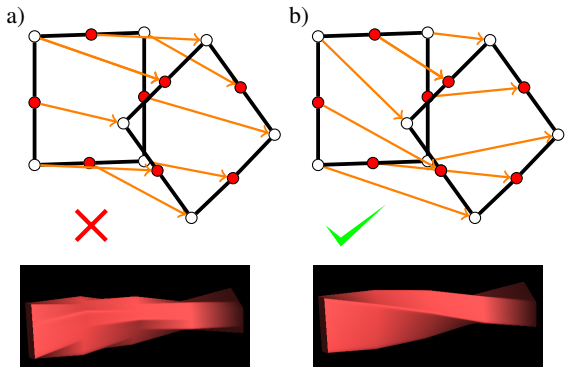

Figure 3: *a) Connecting subsequent cross sections based on closest points may match corner to non-corner points, with undesirable visual results (bottom row). This is avoided by our proposed scheme b).*

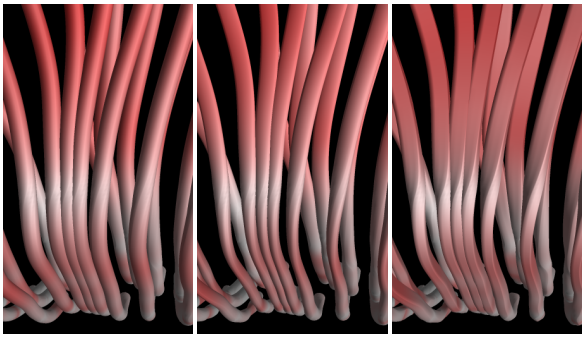

Figure 4: *Compared to streamtubes with a spherical (a) or elliptic cross section (b), the sharp edges of our new superquadric streamtubes (c) most clearly indicate the twisting of medium and minor eigenvector in this example.*

4. Visualizing Uncertainty in HARDI Tractography

Our visualization of the uncertainty in HARDI tractography builds on the HiFiVE descriptor of fiber distributions [SSSSW13]. Tractography follows the mode of that distribution; the anisotropic spread of directions around their mode provides a measure of uncertainty in the propagation direction, which is visualized using our superquadric streamtubes.

4.1. EM Estimation of HiFiVE Descriptors

HiFiVE descriptors summarize the results from N repeated bootstrap estimates of the fiber direction [WTW*08]. When applied to multi-fiber models, each of those N experiments produces a set of k fiber directions. We would like to generate a separate descriptor for each of those k compartments, which requires consistently assigning the results of each experiment to the compartments.

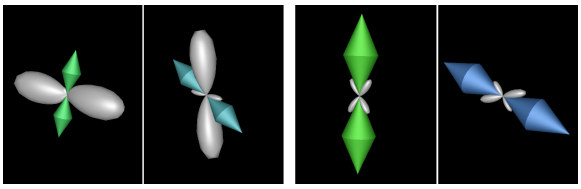

a) b)

Figure 5: *a) Mixing of two similarly strong fiber compartments can greatly inflate the uncertainty estimates in HiFiVE descriptors. b) EM estimation removes this problem.*

In [SSSSW13], this assignment is done based on volume fractions, i.e., in the presence of two fibers, one descriptor summarizes the directions of the dominant fiber, the other one the directions of the secondary fiber. Even though this works well in most cases, it can lead to a mixing of compartments that are similarly strong, since the "dominant" fiber is inconsistent across the N repeats (Figure 5 a).

Therefore, we refine this initial assignment using an expectation-maximization (EM) approach [Bis06]: After first estimating the descriptors, we reassign the k vectors from each experiment so that their joint probability of belonging to the assigned compartments is maximized. This joint probability is easily obtained by adding the results of two inner products, as shown in Eq. (10) of [SSSSW13]. Descriptors are then recomputed based on the modified assignments. This is iterated until assignments no longer change. Convergence is typically reached within few (on average, four) iterations (result in Figure 5 b).

4.2. A Tensor of Propagation Uncertainty

We use the maximum of the fiber distribution as the propagation direction for streamline-based deterministic tractography. We will now derive a 3×3 symmetric positive semidefinite tensor $\mathbf{U}$ that quantifies the uncertainty in this direction. Since the propagation direction is given as a unit vector, there is no uncertainty in its length, so $\mathbf{U}$ has a zero eigenvalue in that direction. The two remaining eigenvectors indicate the principal uncertainties, which we normalize to $[0,1]$.

The uncertainty tensor $\mathbf{U}$ is derived from the Hessian $\mathbf{H}$ of the fiber distribution at its maximum. Since HiFiVEs permit a representation as higher-order tensors, $\mathbf{H}$ can be computed as in Section 4.2 of [SK10a]. We define $\mathbf{U}$ to have the same eigenvectors as $\mathbf{H}$, since they are already aligned with the fiber direction and the principal uncertainties.

In the tangent plane, more strongly negative Hessian eigenvalues μ_i indicate more focused distributions, which implies less uncertainty in the propagation direction. As shown in Appendix A of [SK10a], the smallest possible μ_i, corresponding to a perfectly certain direction, is $-l$, where $l = 8$ is the order of its higher-order tensor representation. Therefore, we can normalize our measure of uncertainty to range $[0,1]$ by mapping the two tangential eigenvalues μ_i to

$$\lambda_i := 1 + \frac{\mu_i}{l}. \tag{3}$$

The superquadric streamtubes in Figure 1 visualize the uncertainty tensor $\mathbf{U}$. Changes in radius illustrate how strongly tracking uncertainty can vary along tracts. In the region of fiber crossing, uncertainty is particularly high in the less dominant compartment. In many places (marked by arrows), streamtubes become flat, indicating that tracking uncertainty is indeed anisotropic. This might be related to fibers that bend or spread mostly within a specific plane.

4.3. Details of the Implementation

Our implementation precomputes HiFiVE descriptors at the corners of each cell. Since this involves fitting multi-fiber models a very large number of times, we use a fast open source implementation of the ball-and-multi-stick model [SWK10]. Since HiFiVEs represent the fiber distributions as members of a function space for which higher-order tensors provide an explicit basis, they can simply be interpolated component wise for tractography [SSSSW13].

In multi-fiber tractography, it is customary to follow the fiber compartment that is most closely aligned with the current tracking direction. In our implementation, we take a weighted average of the descriptors at each cell corner, where the weights are proportional to the probability of the current direction belonging to the respective compartment, and normalized to sum to unity. In most cases, this amounts to selecting the descriptor of the most closely aligned compartment. However, it avoids discontinuities in cases where several compartments align similarly well. Beside the widely used white matter mask and curvature-based termination criteria, we also stop integration when the tracking uncertainty from Eq. (3) exceeds an upper threshold ($\lambda_i > 0.7$).

5. Conclusion

Even though the advantages of superquadric glyphs for tensor visualization [Kin04] are now widely recognized, all streamtube based visualizations we are aware of have used circular or elliptic cross sections [DH93, ZDL03]. Our work closes this gap in the literature by showing how the benefits of superquadric shapes can be transferred to streamtubes. Even though we have focused on an application in which tensor fields are positive definite, it would be straightforward to extend our implementation to indefinite tensors by using a larger part of the superquadric shape space [SK10b].

As a second contribution, we have derived a new propagation uncertainty tensor from the previously described HiFiVE descriptor [SSSSW13], and used it to visualize the uncertainty in HARDI tractography. Unlike previous approaches [JTE*05], the resulting visualization effectively conveys the anisotropic nature of the tracking uncertainty.

References

[BBH14] BROWN C. J., BOOTH B. G., HAMARNEH G.: Uncertainty in tractography via tract confidence regions. In *Computational Diffusion MRI and Brain Connectivity*, Schultz T., Nedjati-Gilani G., Venkataraman A., O'Donnell L., Panagiotaki E., (Eds.). Springer, 2014, pp. 129–138. 2

[Bis06] BISHOP C. M.: *Pattern Recognition and Machine Learning*. Springer, 2006. 4

[BMLB94] BASSER P. J., MATTIELLO J., LE BIHAN D.: Estimation of the effective self-diffusion tensor from the NMR spin echo. *Journal of Magnetic Resonance B*, 103 (1994), 247–254. 1

[BPtHRV13] BRECHEISEN R., PLATEL B., TER HAAR ROMENIJ B. M., VILANOVA A.: Illustrative uncertainty visualization of DTI fiber pathways. *The Visual Computer 29* (2013), 297–309. 2

[BVPtHR09] BRECHEISEN R., VILANOVA A., PLATEL B., TER HAAR ROMENIJ B. M.: Parameter sensitivity visualization for DTI fiber tracking. *IEEE Trans. on Visualization and Computer Graphics 15*, 6 (2009), 1441–1448. 2

[DH93] DELMARCELLE T., HESSELINK L.: Visualizing second-order tensor fields with hyperstreamlines. *IEEE Computer Graphics and Applications 13*, 4 (1993), 25–33. 1, 4

[EBRI09] EVERTS M. H., BEKKER H., ROERDINK J. B. T. M., ISENBERG T.: Depth-dependent halos: Illustrative rendering of dense line data. *IEEE Trans. on Visualization and Computer Graphics 15*, 6 (2009), 1299–1306. 2

[HSSK14] HERMANN M., SCHUNKE A. C., SCHULTZ T., KLEIN R.: A visual analytics approach to study anatomic covariation. In *Proc. IEEE PacificVis* (2014), pp. 161–168. 1

[JKM06] JANKUN-KELLY T. J., MEHTA K.: Superellipsoid-based, real symmetric traceless tensor glyphs motivated by nematic liquid crystal alignment visualization. *IEEE Trans. on Visualization and Computer Graphics 12*, 5 (2006), 1197–1204. 1

[JTE*05] JONES D. K., TRAVIS A. R., EDEN G., PIERPAOLI C., BASSER P. J.: PASTA: pointwise assessment of streamline tractography attributes. *Magnetic Resonance in Medicine 53*, 6 (2005), 1462–1467. 2, 4

[Kin04] KINDLMANN G.: Superquadric tensor glyphs. In *EG/IEEE Symposium on Visualization (SymVis)* (2004), pp. 147–154. 2, 4

[KW06] KINDLMANN G., WESTIN C.-F.: Diffusion tensor visualization with glyph packing. *IEEE Trans. on Visualization and Computer Graphics 12*, 5 (2006), 1329–1335. 1

[KWL*04] KINDLMANN G., WEINSTEIN D., LEE A., TOGA A., THOMPSON P.: Visualization of anatomic covariance tensor fields. In *Proc. IEEE Eng. Med. Biol. Soc.* (2004), pp. 1842–1845. 1

[LG95] LÖFFELMANN H., GRÖLLER E.: Parameterizing superquadrics. *Proc. WSCG'95* (1995), 162–172. 2

[MCCvZ99] MORI S., CRAIN B. J., CHACKO V. P., VAN ZIJL P. C. M.: Three-dimensional tracking of axonal projections in the brain by magnetic resonance imaging. *Annals of Neurology 45*, 2 (1999), 265–269.

[MSE*06] MERHOF D., SONNTAG M., ENDERS F., NIMSKY C., HASTREITER P., GREINER G.: Hybrid visualization for white matter tracts using triangle strips and point sprites. *IEEE Trans. on Visualization and Computer Graphics 12*, 5 (2006), 1181–1188. 2

[PFK07] PETROVIC V., FALLON J., KUESTER F.: Visualizing whole-brain DTI tractography with GPU-based tuboids and LoD management. *IEEE Trans. on Visualization and Computer Graphics 13*, 6 (2007), 1488–1495. 2

[PPvA*11] PRČKOVSKA V., PEETERS T. H. J. M., VAN ALMSICK M., TER HAAR ROMENY B., VILANOVA A.: Fused DTI/HARDI visualization. *IEEE Trans. on Visualization and Computer Graphics 17*, 10 (2011), 1407–1419. 2

[RBE*06] REINA G., BIDMON K., ENDERS F., HASTREITER P., ERTL T.: GPU-based hyperstreamlines for diffusion tensor imaging. In *Proc. Eurographics/IEEE-VGTC Symposium on Visualization (EuroVis)* (2006), Ertl T., Joy K., Santos B., (Eds.), pp. 35–42. 2

[SGS05] STOLL C., GUMHOLD S., SEIDEL H.-P.: Visualization with stylized line primitives. In *Proc. IEEE Visualization* (2005), Silva C., Gröller E., Rushmeier H., (Eds.), pp. 695–702. 2

[SK10a] SCHULTZ T., KINDLMANN G.: A maximum enhancing higher-order tensor glyph. *Computer Graphics Forum 29*, 3 (2010), 1143–1152. 4

[SK10b] SCHULTZ T., KINDLMANN G.: Superquadric glyphs for symmetric second-order tensors. *IEEE Transactions on Visualization and Computer Graphics 16*, 6 (2010), 1595–1604. 4

[SSSSW13] SCHULTZ T., SCHLAFFKE L., SCHÖLKOPF B., SCHMIDT-WILCKE T.: HiFiVE: a hilbert space embedding of fiber variability estimates for uncertainty modeling and visualization. *Computer Graphics Forum 32*, 3 (2013), 121–130. 3, 4

[STS07] SCHULTZ T., THEISEL H., SEIDEL H.-P.: Topological visualization of brain diffusion MRI data. *IEEE Trans. on Visualization and Computer Graphics 13*, 6 (2007), 1496–1503. 2

[SVBK14] SCHULTZ T., VILANOVA A., BRECHEISEN R., KINDLMANN G.: Fuzzy fibers: Uncertainty in dMRI tractography. In *Scientific Visualization: Uncertainty, Multifield, Biomedical, and Scalable Visualization*, Hansen C., Chen M., Johnson C., Kaufman A., Hagen H., (Eds.). Springer, 2014. Preprint: arXiv 1307.3271. 2

[SWK10] SCHULTZ T., WESTIN C.-F., KINDLMANN G.: Multi-diffusion-tensor fitting via spherical deconvolution: A unifying framework. In *Proc. Medical Image Computing and Computer-Assisted Intervention (MICCAI)* (2010), Jiang T., Navab N., Pluim J. P. W., Viergever M. A., (Eds.), vol. 6361 of *LNCS*, Springer, pp. 673–680. 4

[TML11] TOURNIER J.-D., MORI S., LEEMANS A.: Diffusion tensor imaging and beyond. *Magnetic Resonance in Medicine 65*, 6 (2011), 1532–1556. 2

[VVL13] VOS S. B., VIERGEVER M. A., LEEMANS A.: Multi-fiber tractography visualizations for diffusion MRI data. *PLOS ONE 8*, 11 (2013), e81453. 2

[VZKL06] VILANOVA A., ZHANG S., KINDLMANN G., LAIDLAW D. H.: An introduction to visualization of diffusion tensor imaging and its applications. In *Visualization and Processing of Tensor Fields* (2006), Weickert J., Hagen H., (Eds.), Springer, pp. 121–153. 1

[WTW*08] WHITCHER B., TUCH D. S., WISCO J. J., SORENSON A. G., WANG L.: Using the wild bootstrap to quantify uncertainty in DTI. *Human Brain Mapping 29*, 3 (2008), 346–362. 3

[ZDL03] ZHANG S., DEMIRALP C., LAIDLAW D. H.: Visualizing diffusion tensor MR images using streamtubes and streamsurfaces. *IEEE Transactions on Visualization and Computer Graphics 9*, 4 (2003), 454–462. 1, 2, 3, 4